Multi-coset Sampling and Recovery of Sparse Multiband Signals

Michael Lexa, Mike Davies and John Thompson
{michael.lexa,john.thompson,mike.davies}@ed.ac.uk

University of Edinburgh
Institute of Digital Communications
Technical Report

May 2010, Revised October 2010

Abstract

Multi-coset sampling is a periodic nonuniform sub-Nyquist sampling technique for acquiring continuous-time, spectrally sparse signals. This report presents a concise mathematical analysis of the multi-coset sampling system as originally proposed by Feng and Bresler and serves a reference for the accompanying MATLAB software that simulates multi-coset sampling and signal reconstruction. Emphasis is placed on the derivation of the linear relationship between the spectrums of the input and output signals, the conditions of perfect reconstruction, and the reconstruction algorithm.

1 Signal Model and System Description

Sparse multiband signals. A *multiband signal* $x(t)$ is a bandlimited, continuous-time, squared integrable signal that has all of its energy concentrated in one or more disjoint frequency bands (of positive Lebesque measure). Denoting the Fourier transform of $x(t)$ by $X(j\omega)$,

$$X(j\omega) = \int_{-\infty}^{\infty} x(t)\, e^{j\omega t}\; dt,$$

a bandlimited signal is one whose spectrum is bounded, i.e., $X(j\omega) = 0$ for $-\pi W \leq \omega < \pi W$ radians per second, for some positive real number W. Here, $W/2$ is the bandwidth of $x(t)$ and W is therefore the Nyquist frequency. The spectral support of a multiband signal is the union of the frequency intervals that contain the signal's energy. A *sparse* multiband signal is thus a multiband signal whose spectral support has Lebesgue measure that is small relative to the overall signal bandwidth [2]. If, for instance, all the active bands have equal bandwidth B Hz and the signal is composed of K disjoint frequency bands, then a sparse multiband signal is one satisfying $KB \ll W$.

Multi-coset sampler. Multi-coset sampling (MC) is a periodic nonuniform sub-Nyquist sampling technique for acquiring sparse multiband signals [1–5]. For a fixed time interval T that is less than or equal to the Nyquist period and for a suitable positive integer L, MC samplers sample $x(t)$ at the time instants $t = (kL + c_i)T$ for $1 \leq i \leq q$, $k = 0, 1, \ldots$. The time offsets c_i are distinct, positive real numbers less than L and are known collectively as the multi-coset *sampling pattern*. The system thus collects $q \leq L$ samples in LT seconds, or equivalently, exhibits an average sampling rate of q/LT Hz. Here we set T equal to the Nyquist period $T = 1/W$, thereby referencing the system's sampling rate to the Nyquist rate. Multi-coset samplers are parameterized by q, L, and $\{c_i\}$, and the system design depends on conditioning them properly to ensure successful recovery of $x(t)$ from the output samples. MC samplers are most easily implemented as multichannel systems where channel i shifts $x(t)$ by c_i/W seconds and then samples uniformly at W/L Hz (see Figure 1).

2 System Analysis

The following analysis yields a basic time and frequency domain description of the MC sampler. We employ standard Fourier transform properties without explicit explanation for the sake of conciseness.

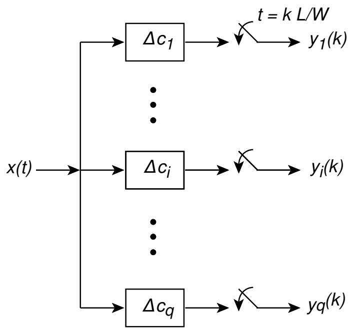

Figure 1: Multi-coset sampler implemented as a multi-channel system. In this case, the base sampling period equals the Nyquist rate W Hz.

The notational style is that of [6]. To denote Fourier transform pairs, we use the shorthand notation,

$$x(t) \overset{\mathrm{FT}}{\longleftrightarrow} X(j\omega),$$

and use the abbrevations FT and DTFT when referring to the Fourier transform and the discrete-time Fourier transform respectively.

2.1 Multi-coset sampling

Let $x(t)$ be a sparse multiband signal. Then by inspection of Figure 1 we have the following time and frequency domain relationships for the i^{th} channel, $i = 1, \ldots, q$.

Shifting in time:

$$x(t + c_i/W) \overset{\mathrm{FT}}{\longleftrightarrow} X(j\omega)e^{j\frac{c_i}{W}\omega}$$

Sampling/Aliasing:

$$\begin{aligned} y_i(k) &= x(kL/W + c_i/W) \\ &\updownarrow \;\; \mathrm{DTFT};\, \tfrac{L}{W} \\ Y_i(e^{j\omega\frac{L}{W}}) &= \frac{W}{L}\sum_{m=\lceil\frac{L}{2}(\frac{\omega}{\pi W}-1)\rceil+1}^{\lfloor\frac{L}{2}(\frac{\omega}{\pi W}+1)\rfloor} X(j\omega - j2\pi\tfrac{W}{L}m)e^{j\frac{c_i}{W}(\omega-2\pi\frac{W}{L}m)} \end{aligned} \tag{1}$$

The summation limits are finite for a given ω because $x(t)$ is assumed bandlimited. Because $Y_i(e^{j\omega\frac{L}{W}})$ is periodic with period $2\pi W/L$, we can, without loss of information, restrict $Y_i(e^{j\omega\frac{L}{W}})$ to one period. Here we choose to restrict ω to $[-\pi W/L, \pi W/L)$ to obtain

$$\begin{aligned} &e^{-j\frac{c_i}{W}\omega}Y_i(e^{j\omega\frac{L}{W}})\mathbf{1}_{[-\frac{\pi W}{L},\frac{\pi W}{L})} = \\ &\frac{W}{L}\sum_{m=-\lfloor\frac{1}{2}(L+1)\rfloor+1}^{\lfloor\frac{1}{2}(L+1)\rfloor} e^{-j\frac{2\pi}{L}c_i m}\, X(\omega - 2\pi\tfrac{W}{L}m)\mathbf{1}_{[-\frac{\pi W}{L},\frac{\pi W}{L})}, \end{aligned}$$

for $i = 1, \ldots, q$, where $\mathbf{1}_{[\cdot)}$ denotes the indicator function. Note that the restriction to $[-\pi W/L, \pi W/L)$ removes the dependence on ω in the summation limits since within this interval $Y_i(e^{j\omega\frac{L}{W}})$ is a linear combination of a particular (finite) set of spectral segments of $x(t)$. We can therefore write this expression in a matrix-vector formulation

$$\mathbf{z}(\omega) = \mathbf{\Phi}\mathbf{s}(\omega) \tag{2}$$

where

$$z_i(\omega) = e^{-j\frac{c_q}{W}\omega} Y_i(e^{j\omega\frac{L}{W}})\mathbf{1}_{[-\frac{\pi W}{L},\frac{\pi W}{L})} \tag{3}$$

$$\mathbf{\Phi}_{i,l} = \frac{W}{L} e^{-j\frac{2\pi}{L}c_i m_l} \tag{4}$$

$$s_l(\omega) = X(\omega - 2\pi\tfrac{W}{L}m_l)\mathbf{1}_{[-\frac{\pi W}{L},\frac{\pi W}{L})} \tag{5}$$

for $i = 1, \ldots, q$, $l = 1, \ldots, L$, and $m_l = -\left\lfloor \frac{1}{2}(L+1) \right\rfloor + l$.

3 Support Recovery and Conditions for Perfect Reconstruction

Support recovery refers to the process of identifying which elements of $\mathbf{s}(\omega)$ contain the active bands that comprise $x(t)$. Since each element of $\mathbf{s}(\omega)$ is a spectral slice of $X(j\omega)$ of width $\frac{W}{L}$ Hz, identifying the active slices can only determine the true band support (bandwidth of the occupied bands) to within a resolution of $\frac{W}{L}$ Hz. Nonetheless, it is important to realize that multi-coset reconstruction will theoretically recover the entire spectrum of $x(t)$.

Support recovery of $\mathbf{s}(\omega)$ is a necessary step in the reconstruction of $x(t)$ because it allows the inversion of the underdetermined linear system in (2). Most of the elements of $\mathbf{s}(\omega)$ will not contain active bands because $x(t)$ is presumed to be spectrally sparse. Thus, if the active elements of $\mathbf{s}(\omega)$ can be identified, it may be possible to sufficiently reduce the dimension of $\mathbf{s}(\omega)$, as well as that of $\mathbf{\Phi}$, such that (2) may be inverted. Support recovery depends on the covariance matrix of the channel outputs and in particular on the covariance matrix's range space. In [1, 2], Feng and Bresler take advantage of the Hermitian symmetry of the covariance matrix and tease out the support using an eigen-decomposition that is similarly used in the well-known MUSIC algorithm [7].

Let $\Omega \subset \{1, \ldots, L\}$ be the index set that marks the locations of the nonzero elements of $\mathbf{s}(\omega)$, $|\Omega| < L$. Recovering the support $\mathbf{s}(\omega)$ means we want to discover Ω. Because $\mathbf{s}(\omega)$ is $|\Omega|$-sparse, $\mathbf{z}(\omega)$ will be a linear combination of only certain columns of $\mathbf{\Phi}$. The index set of these columns is exactly Ω. Thus, if one can identify the active columns of $\mathbf{\Phi}$ (for this given $\mathbf{s}(\omega)$), then we can recover the support of $\mathbf{s}(\omega)$.

Consider the $q \times q$ covariance matrix of $\mathbf{z}(\omega)$,

$$\begin{aligned}\mathbf{R_z} &= \int_{-\pi\frac{W}{L}}^{\pi\frac{W}{L}} \mathbf{z}(\omega)\mathbf{z}^H(\omega)\ d\omega \\ &= \mathbf{\Phi}\left[\int_{-\pi\frac{W}{L}}^{\pi\frac{W}{L}} \mathbf{s}(\omega)\mathbf{s}^H(\omega)\ d\omega\right][\mathbf{\Phi}]^H \\ &= \mathbf{\Phi}\,\mathbf{R_s}\,\mathbf{\Phi}^H,\end{aligned} \tag{6}$$

where H denotes Hermitian transpose and $\mathbf{R_s}$ denotes the covariance matrix of the spectral slices in $\mathbf{s}(\omega)$. Because $\mathbf{s}(\omega)$ is $|\Omega|$-sparse, all but $|\Omega|$ of the rows and columns of $\mathbf{R_s}$ will be zero. This means we can rewrite $\mathbf{R_z}$ using reduced forms of $\mathbf{R_s}$ and $\mathbf{\Phi}$,

$$\mathbf{R_z} = \mathbf{\Phi}_\Omega\,[\mathbf{R_s}]_\Omega\,[\mathbf{\Phi}_\Omega]^H, \tag{7}$$

where $\mathbf{\Phi}_\Omega$ denote the submatrix composed of the columns of $\mathbf{\Phi}$ that are indexed by Ω. If $\text{rank}([\mathbf{R_s}]_\Omega) = |\Omega|$ and if by a suitable choice of the sampling pattern $\text{rank}(\mathbf{\Phi}_\Omega) = |\Omega|$, then (7) implies $\text{rank}(\mathbf{R_z}) = |\Omega|$.

Now consider the eigen-decomposition of $\mathbf{R_z}$, $\mathbf{R_z} = \mathbf{U\Lambda U}^H$, where $\mathbf{U}$ is a matrix of eigenvectors of $\mathbf{R_z}$ and $\mathbf{\Lambda}$ is a diagonal matrix containing the eigenvalues of $\mathbf{R_z}$. Because $\text{rank}(\mathbf{R_z}) = |\Omega|$, $\mathbf{R_z}$ has only $|\Omega|$ nonzero eigenvalues and the eigen-decomposition may be rewritten as

$$\begin{aligned}\mathbf{R_z} &= \mathbf{U}_s\mathbf{\Lambda}_s\mathbf{U}_s^H + \mathbf{U}_n\mathbf{\Lambda}_n\mathbf{U}_n^H \\ &= \mathbf{U}_s\mathbf{\Lambda}_s\mathbf{U}_s^H\end{aligned} \tag{8}$$

where $\mathbf{\Lambda}_s$ and $\mathbf{\Lambda}_n$ are the diagonal matrices containing the nonzero and zero eigenvalues respectively ($\mathbf{\Lambda}_s$ is $|\Omega| \times |\Omega|$), $\mathbf{\Lambda}_n$ is $(q - |\Omega|) \times (q - |\Omega|)$, and $\mathbf{U}_s$ and $\mathbf{U}_n$ are the associated eigenvectors matrices. Equation (8) implies that the columns of $\mathbf{U}_s$ span the same space that the columns of $\mathbf{R_z}$

span, i.e., range($\mathbf{R_z}$) = range($\mathbf{U}_s$) and that the dimension of this space is $|\Omega|$. Because (7) implies range($\mathbf{R_z}$) = range($\mathbf{\Phi}_\Omega$), we have that range($\mathbf{U}_s$) = range($\mathbf{\Phi}_\Omega$). This means that we can identify the active columns of $\mathbf{\Phi}$ by determining which ones lie in the space defined by the columns of $\mathbf{U}_s$. Again, as noted in [2] and [4], this approach is essentially a modified version of the MUSIC algorithm.

Therefore, given $\mathbf{R_z}$, we can take its eigen-decomposition, identify $\mathbf{U}_s$, and project the columns of $\mathbf{\Phi}$ onto the range($\mathbf{U}_s$). If a particular column lies in the range($\mathbf{U}_s$) then this column belongs to $\mathbf{\Phi}_\Omega$, or equivalently, its column index lies in Ω. Perfect support recovery can therefore be (theoretically) achieved for the MC sampler with sparse multiband signals if one has perfect knowledge of $\mathbf{R_z}$, if $\mathbf{R_s}$ has full rank, if $q \geq |\Omega|$, and if every $|\Omega|$ columns of $\mathbf{\Phi}$ are linearly independent. If $\mathbf{R_s}$ is not full rank, then as explained in [2] an approximate solution can be sought through a least squares method.

Once the support is known, (7) can be inverted using a pseudoinverse, provided (7) is a determined or an over determined linear system of equations, i.e. when $q \geq |\Omega|$.

$$\mathbf{s}_\Omega(\omega) = ([\mathbf{\Phi}_\Omega]^T \mathbf{\Phi}_\Omega)^{-1} [\mathbf{\Phi}_\Omega]^T \mathbf{z}(\omega)$$

The pseudoinverse computes the unique least squares solutions to $\mathbf{z}(\omega) = \mathbf{\Phi}_\Omega \mathbf{s}_\Omega(\omega)$, provided that the inverse of the Gram matrix $[\mathbf{\Phi}_\Omega]^T \mathbf{\Phi}_\Omega$ exists [7]. It is well-known that this inverse exists if and only if the columns of $\mathbf{\Phi}_\Omega$ are linearly independent. Furthermore, as is shown in [2], the least squares solution is in this case the true solution and not an estimate because the sparse model $\mathbf{s}_\Omega(\omega)$ (given the correct support Ω) can perfectly explain all the data. Therefore, for the class of $|\Omega|$-sparse multiband signals, necessary and sufficient conditions to ensure a unique solution to *given the correct support* is that the number of measurements q be greater the $|\Omega|$ and that every $|\Omega|$-column submatrix of $\mathbf{\Phi}$ has full rank.

Theorem 1 (Necessary and sufficient conditions for perfect reconstruction)**.** *Let $x(t)$ be a sparse multiband signal with known bandwidth $W/2$ Hz but unknown spectral support. Assume the true covariance matrix $\mathbf{R_z}$ is known and that $\mathbf{R_s}$ has full rank. Then the following conditions are necessary and sufficient to perfectly reconstruct $x(t)$ from its multicoset samples $\mathbf{y}(k)$:*

1. $|\Omega| \leq q \leq L < \infty$
2. *Every $|\Omega|$-column submatrix of $\mathbf{\Phi}$ has full rank*

For the MC sampler, the condition on $\mathbf{\Phi}$ can be ensured by selecting the sampling pattern $\{c_i\}$ appropriately. Feng [2] and Feng and Bresler [1] have found that selecting the c_i's uniformly at random suffice.

As explained below, conditions do exist to correctly recover the support of $\mathbf{s}(\omega)$ in an ideal setting (signal model truly applies and with no noise). However, if the support of all the active slices are not recovered correctly, perfect reconstruction is not possible. If the identified support contains the true support plus some inactive slices, the impact may or may be be significant because, while you will recover all of the active bands, you will also recover segments of the spectrum that only contain noise. The significance of this effect depends on the application.

4 Signal reconstruction

Reconstruction with perfect knowledge of $\mathbf{R_z}$. Then

$$\mathbf{s}_\Omega(\omega) = \mathbf{\Phi}_\Omega^\dagger \mathbf{z}(\omega) \qquad \text{or elementwise} \qquad s_{\Omega,l}(\omega) = \sum_{i=1}^{q} \beta_{l,i} z_i(\omega), \tag{9}$$

where $\mathbf{\Phi}_\Omega^\dagger = \mathbf{\Phi}_\Omega^*(\mathbf{\Phi}_\Omega^* \mathbf{\Phi}_\Omega)^{-1} \mathbf{\Phi}_\Omega$ denotes the pseudoinverse of $\mathbf{\Phi}_\Omega$ and $\beta_{l,i}$ represents the elements of $\mathbf{\Phi}_\Omega^\dagger$.

Because the time domain outputs $y_i(k)$ are readily available, it is convenient to transform (9) into the time domain. Taking the inverse FT, we have

$$s_{\Omega,l}(t) = \frac{1}{2\pi}\int_{-\infty}^{\infty} s_{\Omega,l}(\omega)e^{j\omega t}\, d\omega \tag{10}$$

$$= \frac{1}{2\pi}\int_{-\pi\frac{W}{L}}^{\pi\frac{W}{L}} s_{\Omega,l}(\omega)e^{j\omega t}\, d\omega \tag{11}$$

$$= \frac{1}{2\pi}\sum_{i=1}^{q}\beta_{l,i}\int_{-\pi\frac{W}{L}}^{\pi\frac{W}{L}} z_i(\omega)e^{j\omega t}\, d\omega \tag{12}$$

$$= \frac{1}{2\pi}\sum_{i=1}^{q}\beta_{l,i}\,\frac{L}{W}\int_{-\pi\frac{W}{L}}^{\pi\frac{W}{L}} e^{-j\frac{c_i}{W}\omega}Y_i(e^{j\omega\frac{L}{W}})e^{j\omega t}\, d\omega \tag{13}$$

where (11) follows because $s_{\Omega,l}(\omega)$ is nonzero only on $[-\pi W/L, \pi W/L)$, and (12) and (13) follow from substitutions. From (13), we can derived reconstruction formulae for both the continuous time signal $x(t)$ and the Nyquist samples $x(k/W)$.

To reconstruct $x(t)$ we substitute the definition of the DTFT for $Y_i(e^{j\omega\frac{L}{W}})$ in (13), to obtain

$$s_{\Omega,l}(t) = \frac{1}{2\pi}\sum_{i=1}^{q}\beta_{l,i}\,\frac{L}{W}\int_{-\pi\frac{W}{L}}^{\pi\frac{W}{L}} e^{-j\frac{c_i}{W}\omega}\sum_{m=-\infty}^{\infty} y_i(m)e^{-jm\omega\frac{L}{W}}e^{j\omega t}\, d\omega \tag{14}$$

$$= \frac{1}{2\pi}\sum_{i=1}^{q}\sum_{m=-\infty}^{\infty}\beta_{l,i}\, y_i(m)\int_{-\pi}^{\pi}\exp\left(-j\nu(\tfrac{c_i}{L}+m-\tfrac{W}{L}t)\right)\, d\nu \tag{15}$$

$$= \sum_{i=1}^{q}\sum_{m=-\infty}^{\infty}\beta_{l,i}\, y_i(m)\,\mathrm{sinc}\Big(\pi\big(\tfrac{t-c_i/W}{L/W}-m\big)\Big) \tag{16}$$

The functions $s_{\Omega,l}(t)$ are the time domain equivalents of the spectral slices $\mathbf{s}_\Omega(\omega)$, thus to recover $x(t)$, we shift them in frequency to their appropriate spectral locations,

$$x(t) = \sum_{l\in\Omega}\sum_{i=1}^{q}\sum_{m=-\infty}^{\infty}\beta_{l,i}\, y_i(m)\,\mathrm{sinc}\Big(\pi\big(\tfrac{t-c_i/W}{L/W}-m\big)\Big)\ \exp\left(j2\pi\tfrac{W}{L}lt\right). \tag{17}$$

To reconstruct Nyquist samples, we examine the sampled version of (13),

$$s_{\Omega,l}(k/W) = \frac{1}{2\pi}\sum_{i=1}^{q}\beta_{l,i}\,\frac{L}{W}\int_{-\pi\frac{W}{L}}^{\pi\frac{W}{L}} e^{-j\frac{c_i}{W}\omega}Y_i(e^{j\omega\frac{L}{W}})e^{j\omega\frac{k}{W}}\, d\omega \tag{18}$$

$$= \frac{1}{2\pi}\sum_{i=1}^{q}\beta_{l,i}\int_{-\pi}^{\pi} Y_i(e^{j\nu})e^{-j\frac{c_i}{L}\nu}\, e^{j\frac{k}{L}\nu}\, d\nu \tag{19}$$

$$= \sum_{i=1}^{q}\beta_{l,i}\, y\Big(k-\frac{c_i}{L}\Big), \tag{20}$$

where (19) follows from the substitution $\nu = (L/W)\omega$ and (20) follows from the orthogonality property of the DTFT [6]. Shifting these spectral slices to the appropriate location, we have

$$x(k/W) = \sum_{l\in\Omega}\sum_{i=1}^{q}\beta_{l,i}\, y\Big(k-\frac{c_i}{L}\Big)\ \exp\big(j\frac{2\pi}{L}lk\big) \tag{21}$$

Reconstruction with imperfect knowledge of $\mathbf{R_z}$. To compute the lth row and mth column of $\mathbf{R_z}$, we apply the DTFT orthogonality property [6] to find an expression that involves the output

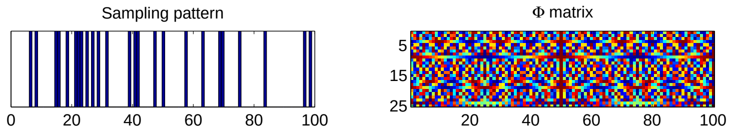

Figure 2: Graphical representation of the sampling pattern and matrix $\mathbf{\Phi}$. For this example, the sampling pattern is chosen uniformly at random from the integers $1, \ldots, L$.

samples $y_i(k)$.

$$[\mathbf{R_z}]_{l,m} = \int_{-\pi\frac{W}{L}}^{\pi\frac{W}{L}} z_l(\omega) z_m^*(\omega)\ d\omega \tag{22}$$

$$= \int_{-\pi\frac{W}{L}}^{\pi\frac{W}{L}} \left[\tfrac{L}{W} e^{-j\frac{c_l}{W}\omega} Y_l(e^{j\omega\frac{L}{W}})\right] \left[\tfrac{L}{W} e^{-j\frac{c_m}{W}\omega} Y_m(e^{j\omega\frac{L}{W}})\right]^*\ d\omega \tag{23}$$

$$= \frac{L}{W} \int_{-\pi}^{\pi} \left[e^{-j\frac{c_l}{L}\nu} Y_l(e^{j\nu})\right] \left[e^{-j\frac{c_m}{L}\nu} Y_m(e^{j\nu})\right]^*\ d\nu \tag{24}$$

$$= 2\pi \frac{L}{W} \sum_{k=-\infty}^{\infty} y_l(k - \frac{c_l}{L}) y_m^*(k - \frac{c_m}{L}), \tag{25}$$

where (24) results from the substitution $\nu = \frac{L}{W}\omega$. Therefore to compute $\mathbf{R_z}$, we need to shift the outputs samples by fractions of the sampling pattern offsets. These fractional shifts are computed by first interpolating $y_i(k)$ by a factor of L and then shifting the resultant signal by the appropriate offsets. Note that (25) indicates an infinite amount of data is needed to compute $\mathbf{R_z}$ exactly. In practice, the best we can do is produce an estimate $\widehat{\mathbf{R}}_\mathbf{z}$ given a finite amount of data,

$$[\widehat{\mathbf{R}}_\mathbf{z}]_{l,m} = 2\pi \frac{L}{W} \sum_{k=0}^{N-1} y_l(k - \frac{c_l}{L}) y_m^*(k - \frac{c_m}{L}), \tag{26}$$

where $N \in \mathbb{Z}^+$. The impact of using only a finite amount of data is beyond the scope of this report, but it does have an impact on the recoverability of the original signal.

5 An Example

The MATLAB scripts accompanying this report were used to simulate the sampling and reconstruction of a sparse multiband signal with three occupied bands, each having bandwidth 10 Hz, with an overall bandwidth of 1000 Hz ($K = 3$, $B = 10$ Hz, $W = 1000$ Hz, center frequencies of bands$= -152, 20, 350$ Hz). We simulated the input by generating a finite sequence of Nyquist samples $x(k/W)$ and had the multi-coset sampler sub-sample this sequence over a simulated period of 20 seconds. The sampler had 25 channels, each of which sampled at 10 Hz ($q = 25$, $\frac{W}{L} = 10$ Hz). The overall simulated sampling rate was $\frac{qW}{L} = 250$ Hz, which is one quarter the Nyquist rate.

Figure 2 graphically displays the sampling pattern used in this example and the matrix $\mathbf{\Phi}$. Figure 4 shows the resulting modified MUSIC spectrum and indicates that four active slices were recovered. In this case, one of the three frequency bands composing $x(t)$ was contained in two spectral slices of $s(\omega)$. Thus the system identified two spectral slices associated with the band centered at -152 Hz, and one slice for each of the bands centered at 20 and 350 Hz, for a total a support of four. This example highlights the fact that multi-coset support recovery can only determine the bandwidth of the the active bands to within a resolution of W/L Hz. Figures 4 and 5 clearly indicate that the Nyquist samples $x(k/W)$ were successfully reconstructed (average-squared error 6.18×10^{-5}).

To demostrate the potential effects of quantization, we performed this example again but quantized the output samples $y_i(k)$ using an eight bit scalar quantizer with a dynamic range of three standard deviations[1]. Figures (6)-(7) show the results.

[1] The term standard deviation is somewhat of a misnomer, because in this report all signals are deterministic. In practical scenarios, however, random noise will most likely be modeled thus making the computation of standard deviations wholly appropriate.

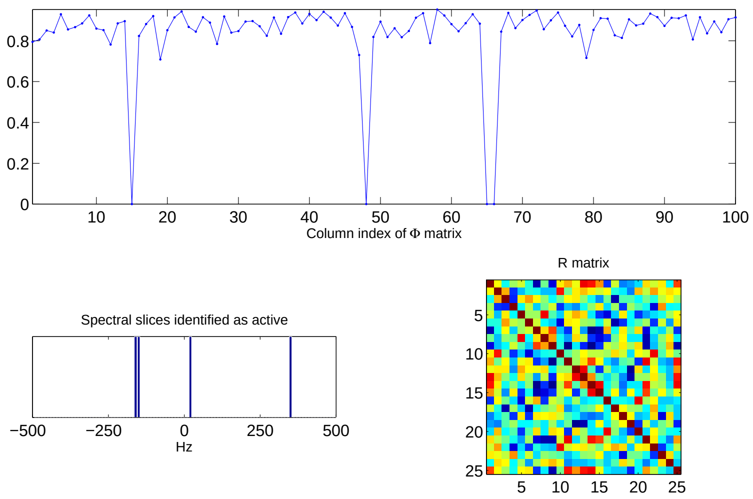

Figure 3: The modified MUSIC spectrum (top panel) clearly identifies four active spectral slices that correspond to the three bands comprising $x(k/W)$. The lower left panel shows the correspondence between the column indices of $\mathbf{\Phi}$ highlighted by the MUSIC spectrum and the center frequencies of the spectral slices. In this case, two of the three bands coincide with the spectral slices, but one band overlaps two spectral slices. Therefore, four spectral slices are identified as active.

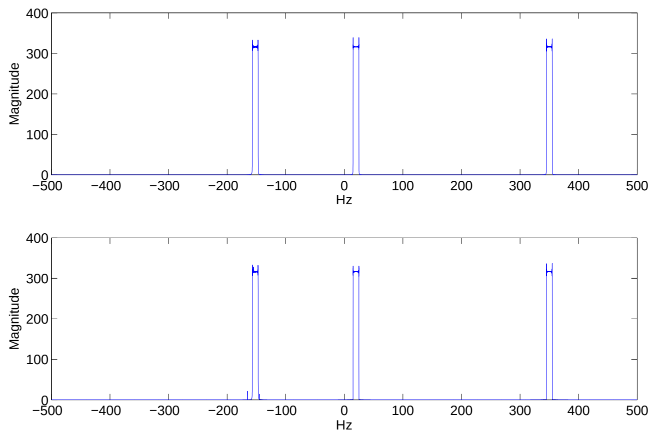

Figure 4: The plots show the frequency spectra of original (top) and recovered (bottom) signals.

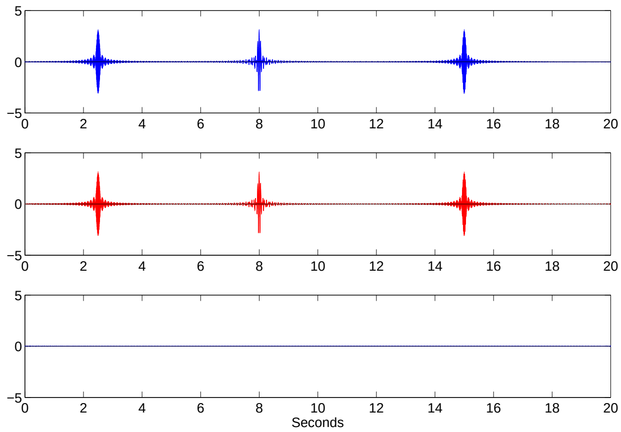

Figure 5: The top and middle panels show the original (blue) and reconstructed (red) signals, respectively. The bottom panel displays the difference signal.

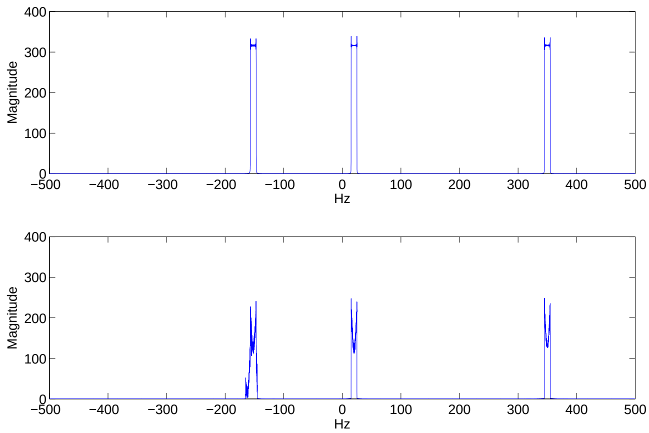

Figure 6: Frequency spectra of the original (top) and recovered (bottom) signals. The lower spectra shows that, in this example, quantization has a significant impact on the spectrum amplitude but does not effect the ability of the system to recover the correct support.

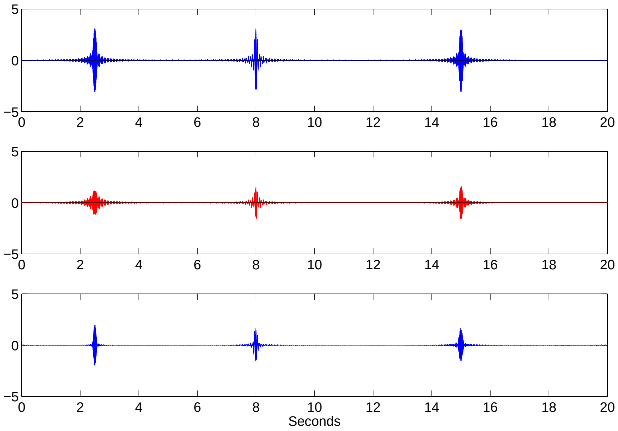

Figure 7: Time domain plots of the original (top) and reconstructed (middle) signals with quantization. The difference signal (bottom) has a average-squared error of 0.0204.

References

[1] P. Feng and Y. Bresler, "Spectrum-blind minimum-rate sampling and reconstruction of multi-band signals," *Proc. IEEE International Conf. on Acoustics, Speech, and Signal Processing*, vol. 3, pp. 1688–1691, May 1996.

[2] Ping Feng, *Universal Minimum-Rate Sampling and Spectrum-Blind Reconstruction for Multiband Signals*, Ph.d., University of Illinois at Urbana-Champaign, Urbana-Champaign, IL U.S.A., 1997.

[3] R. Venkataramani and Y. Bresler, "Perfect reconstruction formulas and bounds on aliasing error in sub-Nyquist nonuniform sampling of multiband signals," *IEEE Trans. Info. Th.*, vol. 46, no. 6, pp. 2173–2183, Sep 2000.

[4] Y. Bresler, "Spectrum-blind sampling and compressive sensing for continuous-index signals," *IEEE Info. Th. and Appl. Workshop*, pp. 547–554, Jan 2008.

[5] M. Mishali and Y. Eldar, "Blind multiband signal reconstruction: Compressed sensing for analog signals," *IEEE Trans. Signal Processing*, vol. 57, no. 3, pp. 993–1009, Mar 2009.

[6] Richard Roberts and Clifford Mullis, *Digital Signal Processing*, Addison-Wesley Publishing Co., Inc., 1987.

[7] L.L. Scharf, *Statistical Signal Processing: Detection, Estimation, and Time Series Analysis*, Addison-Wesley Publishing Co., Reading, MA, 1991.